CONSTRAINTS ON THE THERMAL STATE OF MARS FROM ORBITAL DATA. A. Broquet[1], A.-C. Plesa[2], C. Michaut[3], and M. A. Wieczorek[1], [1]Observatoire de la Côte d'Azur, Laboratoire Lagrange, Université Côte d'Azur, Nice, France (adrien.broquet@oca.eu) [2]German Aerospace Center (DLR), Berlin, Germany, [3]Université de Lyon, Laboratoire de Géologie, Terre, Planète, Environnement, École Normale Supérieur de Lyon, Lyon, France.

Introduction: When a planet's lithosphere is loaded by volcanoes or ice caps, it deviates from its original state and bends. This compensation mechanism gives rise to two principal observables that are detectable from orbit: gravity anomalies, generally measured by Doppler tracking of orbiting spacecraft [1], and topographic expressions, observed by laser altimeters or radar sounders [2].

Analysis of this geodynamical response under stresses imposed by topographic structures of various ages is one of the few methods that give access to the time-integrated strength of the Martian lithosphere [3, 4]. The lithospheric strength is directly linked to the thermal state of the interior and provides important constraints for thermal evolution models of Mars [5, 6].

Current estimates suggest a thin elastic lithosphere (T_e) in the Noachian of about 20 km that rapidly thickens during the Hesperian and Amazonian periods to reach values larger than 300 km at the north pole at present-day [2, 4].

Here, we combine the most recent estimates of T_e beneath the polar caps and volcanic regions with thermal evolution models to build scenarios that describe how Mars could have thermally evolved with time. We determine and discuss key parameters for the thermal evolution models that are able to match T_e estimates.

T_e beneath the polar caps and volcanic regions: T_e beneath the geologically young polar caps ($<$ 10 Ma, [7]) and beneath the older volcanic provinces ($>$ 2 Ga, [8]) have recently been updated by [4, 9].

In [9], the difference between the thickness of the polar cap at a given location based on surface elevations and lithospheric deflection, and a measurement of the polar cap thickness based on radar data was minimized. The minimum T_e beneath the north polar cap was constrained to be 330 km, and was found to be 200 km for the south polar cap, which are consistent with, though higher than, previous studies [2, 10].

T_e in volcanic regions was constrained by [4] using gravity and topography data. This procedure involves matching the observed spectral ratio of the gravity and topography (i.e., the admittance) to a theoretical loading model that predicts the gravity signal based on the observed topography. T_e was found to be less than 30 km beneath Noachian volcanoes, which implies that the lithosphere was weak and hot when they formed.

T_e across the surface using gravity data: Lithospheric properties are expected to vary across the surface of Mars, especially in volcanic regions where heat is concentrated. For this reason, we explored lateral variations in T_e with a localized admittance analysis.

The angular radius and harmonic bandwidth of the localization window were set to 20 in order to maximize the concentration of the window and the number of available harmonic degrees for study. The window was shifted every 5° of longitude and latitude, and the localized admittance was inverted for T_e. The surface density was allowed to vary from 920 (water ice) to 3300 (basalt) kg m^{-3} and other parameters were set following [4]. The range of investigated harmonic degrees was limited to 50 to 80, but it can be shown that varying these does not affect significantly the outcome of our inversions.

Using the geologic map of [11], we obtain a best-fitting mean T_e of 22 (+38,-22) km, 98 (+62,-36) km, and 130 (+62,-68) km for regions with Noachian, Hesperian, and Amazonian surface ages, respectively. We note that these bounds will always underestimate the spatial heterogeneity in T_e at a given epoch because only a limited area for each epoch is available for study at present-day.

In Figure 1, we plot T_e versus the surface age for old volcanoes (circle) and young polar caps (diamond and square). The horizontal lines correspond to the average T_e (black lines) and standard deviation (gray shading) for Noachian, Hesperian, and Amazonian aged surfaces.

We observe that T_e increases with time due to the secular cooling of the planet. T_e in volcanic regions is seen to be generally lower than the Noachian planetary average, given by the horizontal line, and T_e beneath the north polar cap is larger than for the rest of the planet. The lithosphere beneath the south polar cap is seen to be significantly weaker and warmer than at the north [6, 5].

T_e as input to thermal evolution models: To determine how Mars could have thermally evolved with time, we make use of the 130 3-D thermal evolution models of [6]. In [6], the thermal evolution of the interior was modeled by solving the conservation equations of mass, momentum, and energy, and was monitored from 4.5 Gyr ago to present-day.

Several key parameters were varied including the core size, the thickness of the crust (T_c), and the amount and distribution of heat-producing elements (HPE) in the crust and mantle. At any given time and location, it is

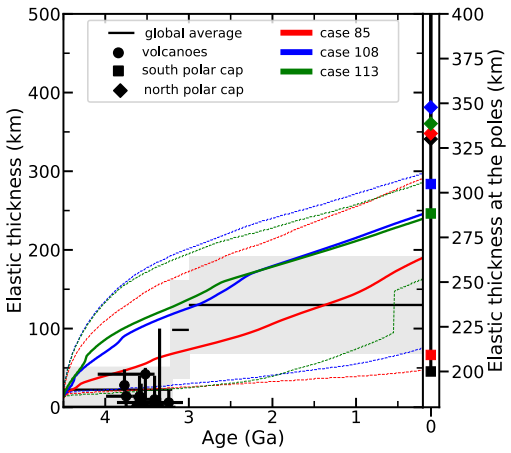

Figure 1: T_e beneath volcanoes (circle), and the north (diamond) and south (square) polar caps as a function of surface age. Average values and standard deviations from global analyses are given for the Noachian, Hesperian, and Amazonian, as horizontal black lines and gray shading. Full range (dashed) and average (solid) T_e from thermal evolution models [6] are plotted for case 85 (red), 108 (blue), 113 (green). From 4.5 to 0.1 Gyr, we use a typical strain rate for mantle convection of 10^{-17} s^{-1}. At present-day (inset), the strain rate is set to 10^{-14} s^{-1}, which corresponds to the polar caps formation timescale.

straightforward to calculate the mechanical thickness of the lithosphere (which is an upper bound for T_e and equal to T_e for zero surface curvature), based on the isotherm that is associated with the onset of ductile deformation [6]. The mechanical thickness can then be compared to the constraints on T_e from orbital data.

Out of the 130 models, 26 models, that all have a core larger than 1700 km [see also, 6], are able to match our constraints on T_e. Amongst them, we identified 3 classes that differ only in terms of T_c and HPE content.

In the first class, as represented by case 85, T_c is 62 km. The crustal heat production rate is given by gamma-ray spectrometer (GRS) data [12], and the bulk silicate abundance of HPEs is given by the compositional model of [13]. In the second class (case 108), T_c is lower, 45 km. The abundance of HPEs in the crust is similar to case 85, but the amount of HPEs in the mantle must be reduced by 30% with respect to case 85. For the third class (case 113), T_c is even lower, 29.5 km. The abundance of HPEs in the mantle is similar to case 85, but the amount of HPEs in the crust is twice that of case 85.

In Figure 1, we show T_e versus surface age as given by the cases 85, 108, and 113. We observe that these 3 different cases match both the range of T_e that are obtained locally for Noachian volcanoes [4] and Amazonian polar caps [9]. They are also in good agreement with the bounds on T_e that were obtained globally for Noachian, Hesperian, and Amazonian epochs. All 3 cases yield similar variation in T_e with time, which tells us that their differences in T_c can be balanced with the concentration of HPEs in the crust or mantle.

Conclusion: As shown by [14], the average value of T_c on Mars can be tightly constrained from gravity and topography data, if T_c is known at one location (e.g., at NASA's InSight landing site). Combining the constraints on T_c from InSight data [15] with estimates of T_e at various locations and epochs will allow to refine thermal evolution models. Since T_e is an indicator of the thermal state of the lithosphere that is sensitive to HPE abundances, orbital constraints on T_e will help us infer the distribution of HPEs between the silicate layers of Mars.

If the average value of T_c is larger than about 60 km, we find cases (e.g., case 85) that match the most recent T_e estimates when using the concentration of HPEs given by GRS data and the bulk silicate abundances from [13]. However, if the average T_c is larger than 87 km (e.g., case 65), then T_e at the south pole is too small with respect to orbital constraints [6]. When T_c is about 45 km on average or lower, the amount of HPEs in the mantle needs to be reduced (case 108) or the crustal abundance in HPEs is required to be significantly higher than the value suggested by GRS data (case 113). In all cases, more than half of the planet's bulk abundance of HPEs is contained in the crust.

We note that cases with a lower amount of HPEs in the mantle may be difficult to reconcile with long-lived volcanic activity in Tharsis and Elysium [e.g., 16, 17].

The full range of crustal parameters that fit our constraints on T_e will be explored using the parametrized model of [5] with two types of crust for the northern and southern hemispheres that have different vertical structures and HPE contents.

References: [1] Genova A. et al. (2016) *Icarus, 272*, 228–245. [2] Phillips R. J. et al. (2008) *Science, 320*, 1182–1185. [3] Grott M. et al. (2013) *Space Sci. Rev., 174*, 49–111. [4] Broquet A. and Wieczorek M.A. (2019) *JGR:Planets,124*, 2054–2086. [5] Thiriet M. et al. (2018) *JGR:Planets,123*, 823–848. [6] Plesa A.-C. et al. (2018) *GRL, 45*, 12,198–12,209. [7] Herkenhoff K. E. and Plaut J. J. (2000) *Icarus, 144*, 243–253. [8] Robbins S. J. et al., (2011) *Icarus, 211*, 1179–1203. [9] Broquet A. et al. (2020) *LPSC LI* [10] Wieczorek M.A. (2008) *Icarus, 196*, 506–517. [11] Tanaka K. L. et al. (2014) [12] Hahn B. C. et al. (2011) *GRL, 38*. [13] Wänke H. et al. (1994) *Roy. Soc., 349*, 285–293. [14] Wieczorek M.A. et al. (2020) *LPSC LI*. [15] Knapmeyer-Endrun B. et al. (2020) *LPSC LI*. [16] Neukum G. et al. (2004) *Nature, 432*, 971–979. [17] Vaucher J. et al. (2009) *Icarus, 204*, 418–442.